



Vacancy induced metallicity at the CaHfO₃/SrTiO₃ interface

Item Type	Article
Authors	Nazir, Safdar;Pulikkotil, Jiji Thomas Joseph;Schwingenschlögl, Udo;Singh, Nirpendra
Citation	Nazir S, Pulikkotil JJ, Singh N, Schwingenschlögl U (2011) Vacancy induced metallicity at the CaHfO ₃ /SrTiO ₃ interface. Appl Phys Lett 98: 133114. doi:10.1063/1.3573808.
Eprint version	Publisher's Version/PDF
DOI	10.1063/1.3573808
Publisher	AIP Publishing
Journal	Applied Physics Letters
Rights	Archived with thanks to Applied Physics Letters
Download date	2023-12-04 17:07:30
Link to Item	http://hdl.handle.net/10754/315751

Vacancy induced metallicity at the CaHfO₃ / SrTiO₃ interface

S. Nazir, J. J. Pulikkotil, N. Singh, and U. Schwingenschlögl

Citation: *Applied Physics Letters* **98**, 133114 (2011); doi: 10.1063/1.3573808

View online: <http://dx.doi.org/10.1063/1.3573808>

View Table of Contents: <http://scitation.aip.org/content/aip/journal/apl/98/13?ver=pdfcov>

Published by the AIP Publishing

The advertisement features a photograph of the Model PS-100 probe station against a blue gradient background. The probe station is a complex piece of equipment with various mechanical components and a central probe tip. The text is arranged around the image: 'NEW' in orange, 'Model PS-100' in large blue font, 'Preconfigured Tabletop Probe Station' in smaller blue font, the Lake Shore CRYOTRONICS logo (a blue square with a white triangle) and name in white, and the tagline 'An affordable solution for a wide range of research' in white script font.

NEW
Model PS-100
Preconfigured Tabletop
Probe Station



Lake Shore
CRYOTRONICS

*An affordable solution for
a wide range of research*

Vacancy induced metallicity at the $\text{CaHfO}_3/\text{SrTiO}_3$ interface

S. Nazir, J. J. Pulikkotil, N. Singh, and U. Schwingenschlög^{a)}

Physical Science and Engineering Division, KAUST, Thuwal 23955-6900, Saudi Arabia

(Received 5 December 2010; accepted 14 March 2011; published online 31 March 2011)

Density functional theory is used to study the electronic properties of the oxide heterointerface $\text{CaHfO}_3/\text{SrTiO}_3$. Structural relaxation is carried out with and without O vacancies. As compared to related interfaces, strongly reduced octahedral distortions are found. Stoichiometric interfaces between the wide band gap insulators CaHfO_3 and SrTiO_3 turn out to exhibit an insulating state. However, interface metallicity is introduced by O vacancies, in agreement with experiment. The reduced octahedral distortions and necessity of O deficiency indicate a less complicated mechanism for the creation of the interfacial electron gas. © 2011 American Institute of Physics.

[doi:[10.1063/1.3573808](https://doi.org/10.1063/1.3573808)]

Heterostructures based on insulating transition metal oxides have acquired a lot of interest ever since it has been reported that a quasi-two-dimensional conducting electron gas can form at the interface. For example, an interface between the two wide band gap insulators LaAlO_3 (LAO) and SrTiO_3 (STO) forms a conducting layer when LAO is grown on the TiO_2 terminated surface of an STO substrate.^{1,2} Various experiments reveal that this interface displays a number of unusual and exciting physical phenomena such as magnetism, magnetoresistance, and superconductivity.³⁻⁶ Presently, its potential for use in nanoelectronic oxide devices is discussed.^{7,8}

Of the three mechanisms proposed to explain the induced metallicity at the interface, the polar catastrophe mechanism seems to hold the upper edge. However, the other two mechanisms, namely, O defects and intersite disorder, also have to be given due consideration. In the polar catastrophe model, the diverging potential which arises from the polar discontinuity at the interface is reflected by an electronic reconstruction of the interface states. In the LAO/STO system, half an electron per areal unit cell is transferred to the n -type $(\text{TiO}_2)^0/(\text{LaO})^+$ interface by partially filling the Ti $3d$ states of the STO conduction band so that the internal electric field is completely compensated. As a result, the interface becomes doped and behaves as a quasi-two-dimensional conducting electron gas. However, for this conductivity mechanism, the multivalent nature of the transition metal ions is quite fundamental. In the LAO/STO system the Ti ions exist in both Ti^{3+} and Ti^{4+} valence states.¹ The polar catastrophe model gives a fairly good estimate of the experimental sheet carrier density. However, it does not explain why interfaces that are grown or annealed at high O partial pressure remain insulating.^{9,10}

Depending on the growth conditions, experiments have found the O sublattice to be nonstoichiometric. Such O defects play a crucial role in determining the transport properties, since it is well known that they are responsible for the metallic behavior of bulk STO. To a certain extent, the interface conductivity, therefore, should be attributed to this bulk mechanism. However, even for defect free interfaces both experiment and theory find conductivity. Hence, also the polar catastrophe mechanism seems to play a role, which may

be complex intertwined. In addition, there exists a third mechanism; the intersite chemical disorder. According to Nakagawa *et al.*,⁵ the formation of the electron gas increases the electric dipole energy, which, however, can be reduced by exchanging Sr with La across the LAO/STO interface. The presence of such disorder has been emphasized in Ref. 11.

Recently, the interface between the two wide band gap insulators CaHfO_3 (~ 5.6 eV band gap) and SrTiO_3 (3.2 eV band gap) was found to show conductivity, but no polar discontinuity was observed.¹² Since Ca and Sr as well as Ti and Hf are isovalent ions, neither the polar catastrophe model nor an intersite chemical disorder can explain the conductivity. The metallic nature consequently hints at O defects, but the mechanism is not yet resolved in detail. In this work, we thus perform a systematic investigation of the $\text{CaHfO}_3/\text{SrTiO}_3$ (CHO/STO) interface. We study the interface relaxation, address the possibility of a critical thickness of the CHO layer, and finally discuss the effects of O vacancies.

Our study relies on density functional theory, applying the full potential linearized augmented plane wave method (WIEN2K package¹³). The electronic exchange correlation potential is parametrized both in the local density approximation (LDA) and the generalized gradient approximation (GGA). The core states are treated fully relativistically, while the scalar relativistic approximation is used for the valence states (the effects of spin-orbit coupling are neglected). We have fully optimized the structures of the different CHO/STO interfaces by relaxing the atomic forces. The lattice constants have been optimized for the two parent compounds. A maximal angular momentum of $l_{\text{max}}=12$ for the wave function expansion in the atomic spheres and a plane wave cutoff of $R_{\text{mt}}, K_{\text{max}}=7.0$ with $G_{\text{max}}=18$ are used. For the interface calculations, we apply a $9 \times 9 \times 2$ k-space grid which contains 30 points within the irreducible wedge of the Brillouin zone. Our basis set consists of the Ca $4s, 3p, 3d$; Sr $5s, 5p$; Hf $6s, 5p, 5d$; Ti $4s, 4p, 3d$; and O $3s, 2p$ valence states. The muffin-tin sphere radii, R_{mt} , (in atomic units) are chosen as 2.5 for both Ca and Sr, 1.98 for both Hf and Ti, and 1.75 for O.

CHO as well as STO crystallize in a cubic structure with space group $Pm\bar{3}m$ (no. 221). The lattice constants are 3.99 Å and 3.905 Å, respectively.^{14,15} Therefore, the lattice mismatch is less than 2%. We first address the structural and electronic properties of the bulk compounds. For LDA and

^{a)}Electronic mail: udo.schwingenschlogl@kaust.edu.sa.

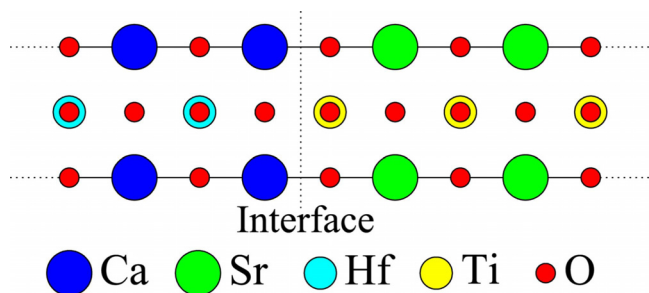


FIG. 1. (Color online) Schematic representation of the CHO/STO interface with the CHO on the left side and the STO on the right side. Large and medium spheres represent Ca/Sr and Hf/Ti atoms, respectively. Small spheres denote O atoms.

GGA, we find CHO lattice constants of 3.95 Å and 4.19 Å, respectively, while for STO they are determined to be 3.87 and 3.99 Å. These results are in good agreement with experiments.^{14,15} The energy gaps of CHO calculated by the LDA and GGA are 3.08 eV and 3.10 eV, respectively, which also agrees well with previous reports.¹⁶ For STO, the LDA and GGA band gaps are 1.85 eV and 1.89 eV, respectively. Even though these values are consistent with previous band structure calculations,¹⁷ the LDA and/or GGA underestimation of the band gap is a well known problem. Since there is little difference between the LDA and GGA results, we use only the LDA in the interface study.

The heterostructures are modeled by setting the lattice constant to the average value of STO and CHO. For all calculations, the STO slab is terminated by the TiO₂ layer. In order to check whether there exists a critical thickness of the CHO slab to impart conductivity, we have carried out calculations for growing thicknesses of the CHO slab on a STO substrate which is 12 unit cells thick. Hence, we investigate (CHO)_n/(STO)₁₂ multilayer systems. The interface structure is illustrated in Fig. 1. Note that for LAO grown on an STO substrate it has been reported that the interface becomes metallic when a critical thickness of four LAO unit cells is

reached.¹⁸ Moreover, it is known that the interface electronic states depend sensitively on structural details,¹⁹ which, therefore, have to be taken into account in the calculation by means of a structure optimization. For the CHO/STO interface, we obtain much less pronounced distortions of the O octahedra as compared to related interfaces, such as LAO/STO. The Ti-O bond lengths change by less than 0.012 Å. Note that we have not taken into account possible effects of octahedral rotations.

Densities of states (DOSs) for (CHO)_n/(STO)₁₂ multilayers of thicknesses $n=1, 2, 3, 4$ are displayed in Fig. 2. Contradicting the experiment,¹² the data show an insulating behavior with a considerable band gap of 1.85 eV before and after the structure relaxation. The same result is obtained for $n=5$ and 6 (not shown) and confirmed for the other configurations under consideration (band gaps between 1.83 and 1.85 eV). We find no systematic change in the DOS as a function of n which would indicate that there exists a critical thickness beyond which the system becomes metallic. The electronic states near the Fermi energy (E_F) mainly trace back to the Ti 3d and O 2p states, while the Hf states are located about 11 eV below E_F . Hence, interface charge transfer and effects of the interface structure relaxation do not play a central role for the metallicity of the CHO/STO interface, in contrast to other perovskite interfaces.^{20,21}

In order to explain the experimental findings, we next introduce O vacancies into both the parent compounds and the heterointerface. The structures are fully relaxed after the introduction of the vacancies. For vacancy studies in oxide interfaces see Refs. 5 and 22, for instance. Our results show that bulk STO becomes metallic by introducing one O vacancy into a $2 \times 2 \times 2$ supercell, which corresponds to an off-stoichiometry of approximately 4%. This finding has already been reported by Djermouni *et al.*²³ In contrast, bulk CHO retains its insulating nature as a consequence of the larger band gap.

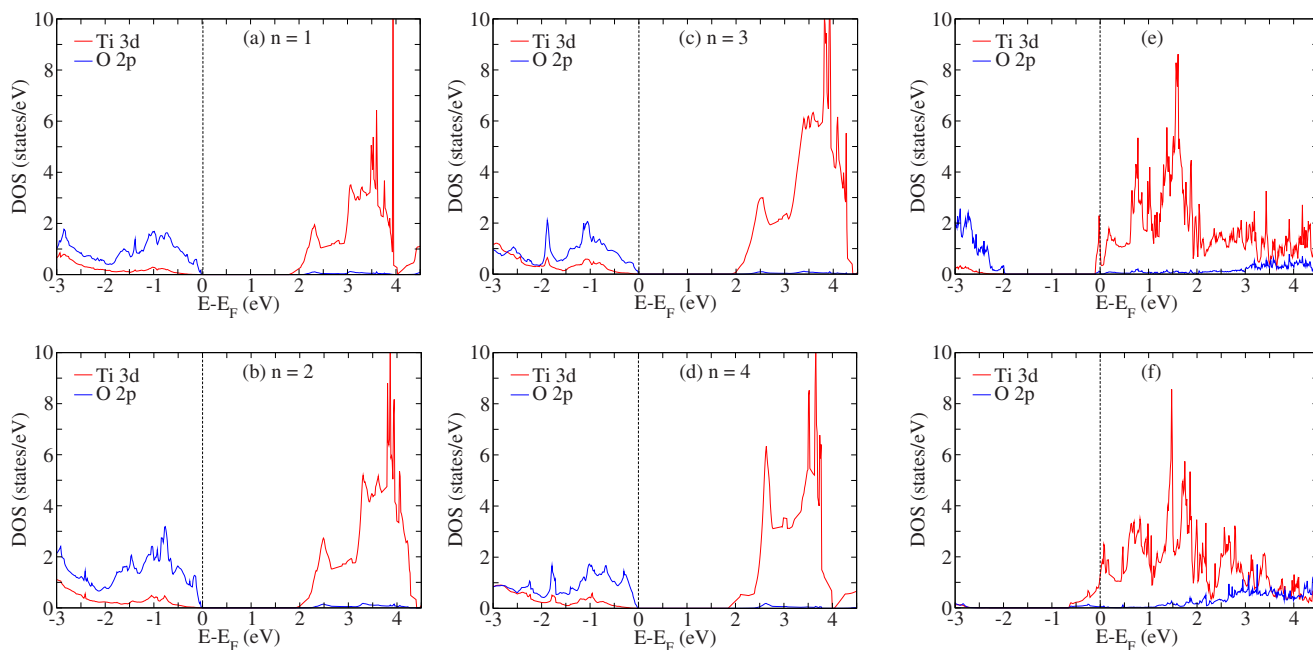


FIG. 2. (Color online) Projected Ti 3d and O 2p DOSs at the interface for the (CHO)_n/(STO)₁₂ heterostructure: [(a)–(d)] without O vacancy, (e) with one O vacancy, and (f) with two O vacancies. In each case the interface structure has been fully relaxed.

We next address the heterointerface by means of a $2 \times 2 \times 6$ supercell which consist of three layers of CHO and three layers of STO. We obtain an insulating state without O vacancies (both with and without structure relaxation). However, metallicity is established by introducing an O vacancy at the interface on the STO side (both with and without structure relaxation). On the right side of Fig. 2 the DOS projected on the Ti $3d$ and O $2p$ states is shown for the relaxed CHO/STO interface, clearly indicating a metallic nature. Therefore, O vacancies on their own can already explain the experimentally observed metallicity.¹² As O deficient bulk CHO stays insulating, it is not surprising that the introduced O vacancy does not result in metallic states on the CHO side of the interface.

Figure 2(e) implies that the metallic states are related to the Ti $3d$ orbitals, which become partially occupied. We conclude that the charge provided by the O vacancy is transferred to the localized Ti $3d$ states. As a consequence, the Ti $3d$ states shift to lower energy, crossing E_F and leaving the interface metallic. The spatial extension of the metallicity perpendicular to the interface is small as the metallic states are strongly suppressed with the distance to the interface. Already the fourth TiO₂ layer is found to be fully insulating.

Moreover, we observe that the metallicity is enhanced when a second O vacancy is added to the CHO/STO interface, see Fig. 2(f). As compared to Fig. 2(e), the chemical potential is shifted significantly toward higher energy, which further increases the occupation of the Ti $3d$ orbitals (rigid band shift). We, therefore, conclude that the metallicity of the interface is the result of O defects and can be controlled by the O partial pressure. If the vacancy is not located at the interface but one atomic layer further away (on the STO side), the interface is still metallic but the number of occupied Ti $3d$ conduction states is reduced significantly to about 10%.

In conclusion, we have studied the metallic conductivity of the CHO/STO interface of wide band gap insulators, which was recently reported.¹² We have applied all electron band structure calculations based on density functional theory. We find for stoichiometric interfaces with CHO layer thicknesses of up to six unit cells as well as for multilayers an insulating state both before and after structure optimization. This result strongly disagrees with the experimental findings. However, it turns out that O vacancies on the STO side of the interface give rise to metallic states, in agreement with the experimental situation.

Therefore, we attribute the CHO/STO interface metallicity to additional charge carriers available for occupying the Ti $3d$ orbitals, which are set free at the O vacancy sites. In fact, we observe that the metallicity is enhanced when the O deficiency grows. The mechanism resulting in metallic states

at the CHO/STO interface appears to be less complex than for many other heterostructures, since there is no polar discontinuity and only a minor structure relaxation, combined with a minimal lattice mismatch. Consequently, the CHO/STO interface has potential in applications of two-dimensional electron gases in nanoelectronic oxide devices, as it will be easier to tailor the properties of the electron gas. However, while the O vacancy concentration can be reliably controlled during growth, a device application additionally requires an environmental control.

We thank KAUST research computing for providing the computational resources used for this investigation.

- ¹A. Ohtomo, D. A. Muller, J. L. Grazul, and H. Y. Hwang, *Nature (London)* **419**, 378 (2002).
- ²A. Ohtomo and H. Y. Hwang, *Nature (London)* **427**, 423 (2004).
- ³N. Reyren, S. Thiel, A. D. Caviglia, L. F. Kourkoutis, G. Hammerl, C. Richter, C. W. Schneider, T. Kopp, A.-S. Rüttschi, D. Jaccard, M. Gabay, D. A. Muller, J.-M. Triscone, and J. Mannhart, *Science* **317**, 1196 (2007).
- ⁴A. Brinkman, M. Huijben, M. van Zalk, J. Huijben, U. Zeitler, J. C. Maan, W. G. van der Wiel, G. Rijnders, D. H. A. Blank, and H. Hilgenkamp, *Nature Mater.* **6**, 493 (2007).
- ⁵N. Nakagawa, H. Y. Hwang, and D. A. Muller, *Nature Mater.* **5**, 204 (2006).
- ⁶S. Okamoto and A. J. Millis, *Nature (London)* **428**, 630 (2004).
- ⁷C. Cen, S. Thiel, G. Hammerl, C. W. Schneider, K. E. Andersen, C. S. Hellberg, J. Mannhart, and J. Levy, *Nature Mater.* **7**, 298 (2008).
- ⁸C. Cen, S. Thiel, J. Mannhart, and J. Levy, *Science* **323**, 1026 (2009).
- ⁹A. Kalabukhov, R. Gunnarsson, J. Börjesson, E. Olsson, T. Claeson, and D. Winkler, *Phys. Rev. B* **75**, 121404(R) (2007).
- ¹⁰G. Herranz, M. Basletić, M. Bibes, C. Carrétéro, E. Tafrat, E. Jacquet, K. Bouzehouane, C. Deranlot, A. Hamzić, J.-M. Broto, A. Barthélémy, and A. Fert, *Phys. Rev. Lett.* **98**, 216803 (2007).
- ¹¹P. R. Willmott, S. A. Pauli, R. Herger, C. M. Schlepütz, D. Martocchia, B. D. Patterson, B. Delley, R. Clarke, D. Kumah, C. Cionca, and Y. Yacoby, *Phys. Rev. Lett.* **99**, 155502 (2007).
- ¹²K. Shibusya, T. Ohnishi, M. Lippmaa, and M. Oshima, *Appl. Phys. Lett.* **91**, 232106 (2007).
- ¹³P. Blaha, K. Schwarz, G. Madsen, D. Kvasnicka, and J. Luitz, *WIEN2k, An Augmented Plane Wave+Local Orbitals Program for Calculating Crystal Properties* (Technical University of Vienna, Vienna, 2001).
- ¹⁴A. S. Verma and V. K. Jindal, *J. Alloys Compd.* **485**, 514 (2009).
- ¹⁵C. Lasota, C. Z. Wang, R. Yu, and H. Krakauer, *Ferroelectrics* **194**, 109 (1997).
- ¹⁶D. Cherrad, D. Maoche, M. Reffas, and A. Benamrani, *Solid State Commun.* **150**, 350 (2010).
- ¹⁷K. van Benthem, C. Elsässer, and R. H. French, *J. Appl. Phys.* **90**, 6156 (2001).
- ¹⁸S. Thiel, G. Hammerl, A. Schmehl, C. W. Schneider, and J. Mannhart, *Science* **313**, 1942 (2006).
- ¹⁹U. Schwingenschlögl and C. Schuster, *EPL* **86**, 27005 (2009).
- ²⁰U. Schwingenschlögl and C. Schuster, *EPL* **81**, 17007 (2008).
- ²¹U. Schwingenschlögl and C. Schuster, *Chem. Phys. Lett.* **467**, 354 (2009).
- ²²M. S. Park, S. H. Rhim, and A. J. Freeman, *Phys. Rev. B* **74**, 205416 (2006).
- ²³M. Djermouni, A. Zaoui, S. Kacimi, and B. Bouhafs, *Comput. Mater. Sci.* **49**, 904 (2010).